Journal of Gerontology: BIOLOGICAL SCIENCES
Cite journal as: J Gerontol A Biol Sci Med Sci. 2011 December;66A(12):1286–1299
doi:10.1093/gerona/glr125

Advance Access published on August 26, 2011

Thioredoxin 1 Overexpression Extends Mainly the Earlier Part of Life Span in Mice

Viviana I. Pérez,[1,2] Lisa A. Cortez,[1] Christie M. Lew,[1] Marisela Rodriguez,[1] Celeste R. Webb,[1] Holly Van Remmen,[1,2,3] Asish Chaudhuri,[1,3,4] Wenbo Qi,[1] Shuko Lee,[3] Alex Bokov,[1,5] Wilson Fok,[2] Dean Jones,[6] Arlan Richardson,[1,2,3] Junji Yodoi,[7] Yiqiang Zhang,[1] Kaoru Tominaga,[1,2] Gene B. Hubbard,[1,8] and Yuji Ikeno[1,3,8]

[1]Barshop Institute for Longevity and Aging Studies and [2]Department of Cellular and Structural Biology, University of Texas Health Science Center at San Antonio.
[3]Research Service, Audie Murphy VA Hospital South Texas Veterans Health Care System, San Antonio.
[4]Department of Biochemistry and [5]Department of Epidemiology and Biostatistics, University of Texas Health Science Center at San Antonio.
[6]Division of Pulmonary, Allergy and Critical Care Medicine, Clinical Biomarkers Laboratory, Department of Medicine, Emory University School of Medicine, Atlanta, Georgia.
[7]Department of Biological Responses, Institute for Virus Research, Kyoto University, Kyoto, Japan.
[8]Department of Pathology, University of Texas Health Science Center at San Antonio.

Address correspondence to Yuji Ikeno, MD, PhD, Barshop Institute for Longevity and Aging Studies, University of Texas Health Science Center at San Antonio, 15355 Lambda Drive, San Antonio, TX 78245-3207. Email: ikeno@uthscsa.edu

We examined the effects of increased levels of thioredoxin 1 (Trx1) on resistance to oxidative stress and aging in transgenic mice overexpressing Trx1 [Tg(*TRX1*)$^{+/0}$]. The Tg(*TRX1*)$^{+/0}$ mice showed significantly higher Trx1 protein levels in all the tissues examined compared with the wild-type littermates. Oxidative damage to proteins and levels of lipid peroxidation were significantly lower in the livers of Tg(*TRX1*)$^{+/0}$ mice compared with wild-type littermates. The survival study demonstrated that male Tg(*TRX1*)$^{+/0}$ mice significantly extended the earlier part of life span compared with wild-type littermates, but no significant life extension was observed in females. Neither male nor female Tg(*TRX1*)$^{+/0}$ mice showed changes in maximum life span. Our findings suggested that the increased levels of Trx1 in the Tg(*TRX1*)$^{+/0}$ mice were correlated to increased resistance to oxidative stress, which could be beneficial in the earlier part of life span but not the maximum life span in the C57BL/6 mice.

Key Words: Thioredoxin—Transgenic mouse—Oxidative stress—Protein carbonylation—Aging.

Received February 14, 2011; Accepted July 6, 2011

Decision Editor: Rafael de Cabo, PhD

THIOREDOXIN (Trx) is a small protein (12 kDa) with two redox-active cysteine residues in the active center (Cys-Gly-Pro-Cys) and was first recognized in the early 1960s as the reductant for a variety of enzymes. Isoforms of Trx have been found in *Escherichia coli*, yeast, and mammals. Two Trxs have been identified in humans, one cytosolic (Trx1) (1) and one mitochondrial (Trx2) (2). Knockout mice for either Trx1 or Trx2 are embryonic lethal (3,4), which demonstrates the essential roles of Trx1 and Trx2 in mammals. A major role of Trx is as a hydrogen donor for enzymes involved in reductive reactions, for example, ribonucleotide reductase, which reduces ribonucleotides to deoxyribonucleotides for DNA synthesis; peroxiredoxins (Prxs), which reduce peroxides (5–7); and methionine sulfoxide reductases, which reduce methionine sulfoxide in proteins and provide protection against oxidative stress (8–10). In addition, Trx protects cells and tissues from oxidative stress (11). Trx1 also plays an important role in maintaining the reduced environment in the cells, which maintains cysteine residues in protein in a reduced state (12). Because the thiol-disulfide exchange reactions are rapid and readily reversible, this reaction is ideally suited to control protein function via the redox state. This is particularly important for several transcription factors, such as AP-1 and NFκB, that contain cysteine residues (13–15). The reduction of cysteine residues increases the DNA-binding activity of these transcription factors (14,15), which subsequently induce the expression of target genes. Furthermore, Trx1 has antiapoptotic effects through the inhibition of the apoptosis signaling kinase (ASK) pathway (16).

Previous studies in *Caenorhabditis elegans* and *Drosophila* indicate that Trx plays roles in oxidative stress and longevity (17,18). In mice, the overexpression of Trx1 resulted in resistance to ischemic injury and lower levels of protein oxidation in brain tissue (11). A previous study demonstrated that Trx1 transgenic mice [Tg(*TRX1*)$^{+/0}$] have an increased life span compared with their wild-type (WT) littermates (19,20); however, the results of this study were compromised by the short life span of the control mice.

The purpose of this study therefore was to determine whether increased levels of Trx1 alter the resistance to endogenous oxidative damage under both normal and induced conditions and if the resistance to oxidative stress by Trx1 could extend life span using the transgenic mice that overexpress thioredoxin 1 [Tg(*TRX1*)$^{+/0}$ mice]. To explore the protective role of Trx1 against endogenous oxidative damage and its long-term pathophysiological consequences, we further characterized the Tg(*TRX1*)$^{+/0}$ mice, measuring the Trx1 expression, levels of Trx2 and glutaredoxin, major antioxidant enzyme activities, levels of protein carbonylation, and sensitivity to oxidative stress induced by diquat administration in young Tg(*TRX1*)$^{+/0}$ and WT mice. Furthermore, we compared the longevity and end-of-life pathology of Tg(*TRX1*)$^{+/0}$ and WT mice. We report that the increased levels of Trx1 in the Tg(*TRX1*)$^{+/0}$ mice were correlated to reduced oxidative damage to protein and lipid, thereby increasing resistance to endogenous oxidative stress and maintaining the redox state in vivo and were beneficial to the survival in the earlier part of life span in the C57BL/6 mice.

Methods

Animals and Animal Husbandry

The Trx1 transgenic mice used in this study were generated using the human TRX1 complementary DNA (cDNA) fused to the β-actin promoter (11). These transgenic mice were produced in the C57BL/6 genetic background. Male hemizygous transgenic mice [Tg(*TRX1*)$^{+/0}$] were crossed to C57BL/6J females to generate hemizygous transgenic and WT control mice. All mice were fed a commercial chow (Teklad Diet LM485, Madison, WI) and acidified (pH = 2.6–2.7) filtered reverse osmosis water ad libitum. To measure the amount of food consumption, the amount of chow removed from the cage hopper and the spillage (the chow on the bottom of the cage) were weighed monthly. Actual food consumed was calculated by subtracting the spillage from the chow removed from the hopper. All the mice were weighed monthly. The mice were maintained pathogen free in microisolater units on Tek FRESH ultra laboratory bedding. Sentinel mice housed in the same room and exposed weekly to bedding collected from the cages of experimental mice were sacrificed on receipt and every 6 months thereafter for monitoring of viral antibodies (Mouse Level II Complete Antibody Profile CARB, Ectro, EDIM, GDVII, LCM, M. Ad-FL, M. Ad-K87, MCMV, MHV, *M. pul.*, MPV, MVM, Polyoma, PVM, Reo, Sendai; BioReliance, Rockville, MD). All tests were negative. For the experiments, three age groups were used: young (4–6 months old), middle (14–16 months old), and old (26–28 months old).

Determination of Trx1 Expression and Activities and Thioredoxin Reductase Activities

Cytosolic fractions obtained from tissues homogenized in ice-cold lysis buffer (2 mM Tris, pH 7.4, 0.05% sodium dodecyl sulfate) and centrifuged for 10 minutes at 10,000*g* at 4°C were used to determine Trx1 levels in several tissues obtained from Tg(*TRX1*)$^{+/0}$ and WT mice by Western blot analysis using goat anti-human Trx1 polyclonal antibodies (Cat. #705; American Diagnostica, Inc., Greenwich, CT). These antibodies recognize total Trx1 (both oxidized and reduced forms). After incubation with the primary antibody, membranes were incubated with the peroxidase-linked secondary antibody (Cat. #P0449; Dako, Carpinteria, CA). Chemiluminescence was detected with an ECL Western blot detection kit (Amersham Biosciences Corp., Piscataway, NJ). The biological activity of Trx was measured in homogenates using the activity assay previously described by Holmgren (21). Trx activity was measured by quantization of thiol groups by DTNB [5,5′-dithiobis(2-nitrobenzoic acid)] following the absorbance at 412 nm. Thioredoxin reductase (TrxR) activity was measured in the presence of thioredoxin-S2 and NADPH. The reaction was followed by recording the increase in absorbance at 340 nm at 0.5-minute intervals.

Measurement of Redox Status of Trx1 and GSH in Livers From Tg(TRX1)$^{+/0}$ and WT Mice

The redox measurements of Trx1 were performed based on a method described by Ritz and Beckwith (22) and Halvey and colleagues (23) with some modifications. Liver tissues were homogenized in 20 mM Tris, pH 8.0, containing 15 mM 4-acetoamido-4′-maleimidylstilbene-2,2′-disulfonic acid (AMS; Molecular Probes, Eugene, OR), supplemented with protease cocktail inhibitor III (Calbiochem, La Jolla, CA). The homogenates were centrifuged at 100,000*g* for 60 minutes at 4°C to obtain the cytosolic fractions. The cytosolic fractions (1 mg/mL) were incubated with 15 mM of AMS in 20 mM Tris, pH.8.0, for 3 hours at room temperature in the dark. The excess of AMS was removed using Microcon YM-3 (Millipore Corporation, Billerica, MA). Trx1 redox forms were separated on a sodium dodecyl sulfate/15% polyacrylamide gel under nonreducing conditions. The gel was electroblotted onto a nitrocellulose membrane, and the membrane was probed with a Trx1 polyclonal antibody obtained from American Diagnostica, Inc. (22,23).

The levels of GSH/GSSG and CySH/CyS-S were measured in liver and blood samples described previously by Jones and colleagues (24). Briefly, 50 μL of fresh blood were mixed with 500 μL of solution A (100 mM serine·borate [pH 8.5] containing [per milliliter] 0.5 mg sodium heparin, 1 mg bathophenanthroline disulfonate sodium salt, and 2 mg iodoacetic acid) and gently inverted twice for mixing. The tubes were then spun in a microcentrifuge for 30 seconds to remove blood cells. Then 200 μL of supernatant from the A tubes were transferred to B tubes (10% [w/v] perchloric acid (PCA) containing 0.2 M boric acid and 10 μM γ-Glu-Glu), and the tubes were inverted to mix. Collected samples were

placed at −80°C as soon as possible for storage. Fifty milligrams of frozen liver were homogenized in 0.5 mL of 5% PCA/0.2 M boric acid/10 uM r-EE solution provided by Clinical Biomarkers Lab (Jones Lab, Emory University). Samples were sonicated to breakdown any aggregates and were then clarified by centrifugation at 10,000*g* for 5 minutes. The supernatants (300 µL) were stored at −80°C. The levels of reduced and oxidized forms of gluthathione and cysteines in liver samples were detected at the nanomoles level using N-dansyl derivatives and high-performance liquid chromatography with fluorescence detection (24).

Thioredoxin 2 and Glutaredoxin Levels

Thioredoxin 2 (Trx2) and glutaredoxin (Grx) levels were measured using mitochondrial and total homogenate fractions (for Trx2 and glutaredoxin, respectively) obtained from the livers of Tg(*TRX1*)$^{+/0}$ and WT mice as previously described (25). Western blot analysis was performed using goat antihuman glutaredoxin polyclonal antibody (Cat. #710; American Diagnostica, Inc.) and rabbit anti-Trx2 polyclonal antibody (Cat. #LF-PA0012; LabFrontier, Seoul, Korea). After incubation with the primary antibodies, membranes were incubated with the respective peroxidase-linked secondary antibodies (Cat. #P0449 and #P0217; Dako). Chemiluminescence was detected using the ECL Western blot detection kit (Amersham Biosciences Corp.).

Determination of the Activity of Major Antioxidant Enzymes: Cu/ZnSOD, MnSOD, Glutathione Peroxidase, and Catalase

The activities of major antioxidant enzymes (Cu/ZnSOD, MnSOD, glutathione peroxidase [Gpx], and catalase) were measured in tissue homogenates from Tg(*TRX1*)$^{+/0}$ and WT mice. The supernatants were used for the antioxidant defense enzymatic activity assay. Gpx activity in tissue homogenates was measured by the assay as described by Sun and colleagues (26). Catalase activity was determined by measuring the decomposition of hydrogen peroxide at 520 nm using the Catalase-520 assay kit (*Oxis*Research, Portland, OR). MnSOD and Cu/ZnSOD levels were measured by activity gels as previously described (27). The images of the gels were analyzed by ImageQuant software.

Assays for Oxidative Damage to Proteins

The levels of protein carbonyl groups were measured using a fluorescence-based assay developed by Chaudhuri and colleagues (28). This assay uses the fluorescein derivative with a hydrazine moiety. The high fluorescence quantum yield of the fluorescein moiety allows the detection of specific proteins that have low levels of protein carbonyls or low abundance proteins with carbonyl groups. The levels of protein carbonyl are expressed as fluorescence units (FU) milligram protein. Cysteine oxidation was measured using a chemical method to detect the presence of disulfides (29). Liver tissues were homogenized in 50 mM potassium phosphate buffer pH 8.0 containing 150 mM iodoacetamide to prevent artifactual generation of disulfide linkages. The free iodoacetamide was removed by protein precipitation with 10% TCA, and the samples were resuspended in 8 M urea and incubated with dithiothreitol (DTT) to reduce disulfide bonds in the samples. Free thiol groups (–SH) arising from the reduced disulfides were labeled with 6-iodoacetamidofluorescein (6-IAF, 1 mM), a fluorescent-tagged iodoacetamide that can accurately quantify the disulfide bonds in proteins. The data are expressed as fluorescence units (FU)/milligram of protein.

Assays for Lipid Peroxidation (F2-isoprostane levels)

The levels of F2-isoprostanes were determined using gas chromatography/mass spectrometry as described by Morrow and Roberts (30). Plasma was added to high-performance liquid chromatography (pH 3.0) water and mixed by vortex. After centrifugation (2,500*g* for 3 minutes at 4°C), the F2-isoprostanes were extracted from the clear supernatants with a C18 Sep-Pak column and a silica Sep-Pak column. The F2-isoprostanes were then converted to pentafluorobenzyl esters and subjected to thin layer chromatography. The F2-isoprostanes were further converted to trimethysilyl ether derivatives, and the F2-isoprostanes levels were quantified by gas chromatography and mass spectrometry. An internal standard, 8-isoPGF2a-d4 (Cayman Chemical, Ann Arbor, MI), was added to the samples at the beginning of extraction to correct the yield of the extraction process. The amount of F2-isoprostanes is expressed as picograms of 8-Iso-prostaglandin F2 per milliliter of plasma.

Assays for DNA Oxidation (8-oxodG levels)

The levels of oxidative damage to DNA were measured by the amount of 8-oxo-2-deoxyguanosine (oxo8dG) in DNA as described by Hamilton and colleagues (31). DNA was isolated from liver tissue by NaI extraction using the DNA Extractor WB Kit (Wako Chemicals USA, Inc., Richmond, VA). The data are expressed as the ratio of nanomoles of oxo8dG to 10^5 nmoles of 2dG.

Diquat Administration and Measurement of Plasma Alanine Aminotransferase (ALT) levels

Two groups of Tg(*TRX1*)$^{+/0}$ and WT mice (4–6 months of age) were injected intraperitoneally with diquat dissolved in saline at doses of 50 or 60 mg/kg. The mice were injected with diquat at a dose of 50 mg/kg and were sacrificed 6 hours after injection, and then the plasma was collected to determine ALT activity. Plasma ALT activities were determined using an ALT kit (SGPT; Teco Diagnostics, Anaheim, CA). Injection of 60 mg/kg diquat was used in generating the survival curves for the young (4–6 months of age)

Tg(*TRX1*)$^{+/0}$ and WT mice. Survival experiment was conducted with 15 male WT and 30 male Tg(*TRX1*)$^{+/0}$ mice.

Determination of ASK1 and NFκB Signaling Pathway Activity

Levels of JNK (phosphorylated and nonphosphorylated forms) were measured in the liver cytosolic fractions of Tg(*TRX1*)$^{+/0}$ and WT mice by Western blot analysis using mouse JNK (Cat. #3708) and phospho-JNK (Thr183/Tyr185: Cat. #9251) antibodies (Cell Signaling Technology, Inc., Santa Cruz, CA).

For immunoprecipitation, the lysates were incubated with goat anti-ASK1 antibody (Cat. #sc-6368, Santa Cruz Biotechnology, Inc., Santa Cruz, CA) at 4°C overnight. Then, protein A Sepharose beads (GE Healthcare Bio-Science, Pittsburgh, PA) were added and incubated an another 1 hour at 4°C. The beads were washed four times with lysis buffer, resuspended in sodium dodecyl sulfate sample buffer, and boiled for 3 minutes. Samples were loaded onto sodium dodecyl sulfate–polyacrylamide gel electrophoresis, and the separated proteins were transferred onto nitrocellulose membrane. ASK1-bound Trx1 and precipitated ASK1 were detected with goat antihuman Trx1 polyclonal (Cat. # 705; American Diagnostica, Inc.) and anti-ASK1 polyclonal antibodies, respectively. The membrane was incubated with primary antibody following incubation with horseradish peroxidase–conjugated secondary, and then the proteins were detected using ECL Western Blotting Detection System.

Expression of some of the NFκB target genes were measured using quantitative real-time polymerase chain reaction (qRT-PCR). Approximately 100 mg of liver tissue was used for RNA extraction employing the RNAqueous kit (Ambion, Inc., Foster City, CA) according to the manufacturer's protocol and then was treated with Turbo-free DNase (Ambion, Inc.) to remove any DNA contamination. Quality of RNA was assessed by agarose gel and quantified by ultraviolet spectrophotometer at 260 nm. The ratio of 260/280 nm was used to assess any DNA contamination. One microgram of RNA was then reverse transcribed using the Retroscript kit (Ambion, Inc.) to obtain the cDNA following the manufacturer's protocol. Each RNA sample was monitored for genomic DNA contamination by a reaction mix without reverse transcriptase addition. All cDNAs were diluted to 1, 1:10, and 1:100 before being used as PCR templates. Primers were designed using Primer Express (Applied Biosystem, Inc., Foster City, CA). qRT-PCR was performed using SYBR Green PCR Master Mix (Applied Biosystem, Inc.). The following primer pairs were used: Interleukin (IL)-1β: forward primer 5′-TCCCCAACTGGTACATCAGCA-3′and reverse primer 5′-CACGGATTCCATGGTGAAGTC-3′; CCl5: forward primer 5′-ATATGGCTCGGACACCACTC-3′ and reverse primer 5′-GTGACAAACACGACTGCAAGA-3′; and tumor necrosis factor (TNF) α: forward primer 5′-CATCTTCTCAAAATTCGAGTGACAA-3′ and reverse primer 5′-TGGGAGTAGACAAGGTACAACCC-3′. qRT-PCR assays for each gene target were performed on cDNA samples and the housekeeping standard GAPDH in 96-well optical plates by a 7500 Real-Time PCR Detection System (Applied Biosystem, Inc.).

Survival Study

Mice in the survival groups were allowed to live out their life, and the life span for individual mice was determined by recording the age of spontaneous death. Two survival studies were conducted using different cohorts; first cohort consists of 48 male WT and 41 male Tg(*TRX1*)$^{+/0}$ mice, and the second cohort consists of 60 male WT and 60 male Tg(*TRX1*)$^{+/0}$ mice and 40 female WT and 40 female Tg(*TRX1*)$^{+/0}$ mice. The survival curves were compared statistically using the log-rank test (32). Median, mean, 90th, 75th, 25th, and 10th percentile (when 10%, 25%, 75%, or 90% of the mice died), and maximum survivals were calculated for each group. Mean survivals for each experimental group were compared with the respective WT group by performing a Student's *t* test upon log-transformed survival times. The median, 10th, 25th, 75th, and 90th percentile survivals for each group were compared with the WT group using a score test adapted from Wang and colleagues (33).

Pathological Assessment

After mice were necropsied for gross pathological lesions, the following organs and tissues were excised and preserved in 10% buffered formalin: brain, pituitary gland, heart, lung, trachea, thymus, aorta, esophagus, stomach, small intestine, colon, liver, pancreas, spleen, kidneys, urinary bladder, reproductive system (male: prostate, testes, epididymis, and seminal vesicles and females: ovaries, oviduct, uterus, and vagina), thyroid gland, adrenal glands, parathyroid glands, psoas muscle, knee joint, sternum, and vertebrae. Any other tissues with gross lesions were also excised. The fixed tissues were processed conventionally, embedded in paraffin, sectioned at 5 μm, and stained with hematoxylin–eosin. Although autolysis of varying severity occurred, it did not prevent the histopathological evaluation of lesions, with the exception of three mice. Diagnosis of each histopathological change was made with histological classifications in aging mice previously described (34,35). A list of pathological lesions was constructed for each mouse that included both neoplastic and nonneoplastic diseases. Based on these histopathological data, the probable cause of death in each mouse was assessed.

Statistical Analysis

Unless otherwise specified, all experiments were done at least in triplicate. Data were expressed as means ± standard

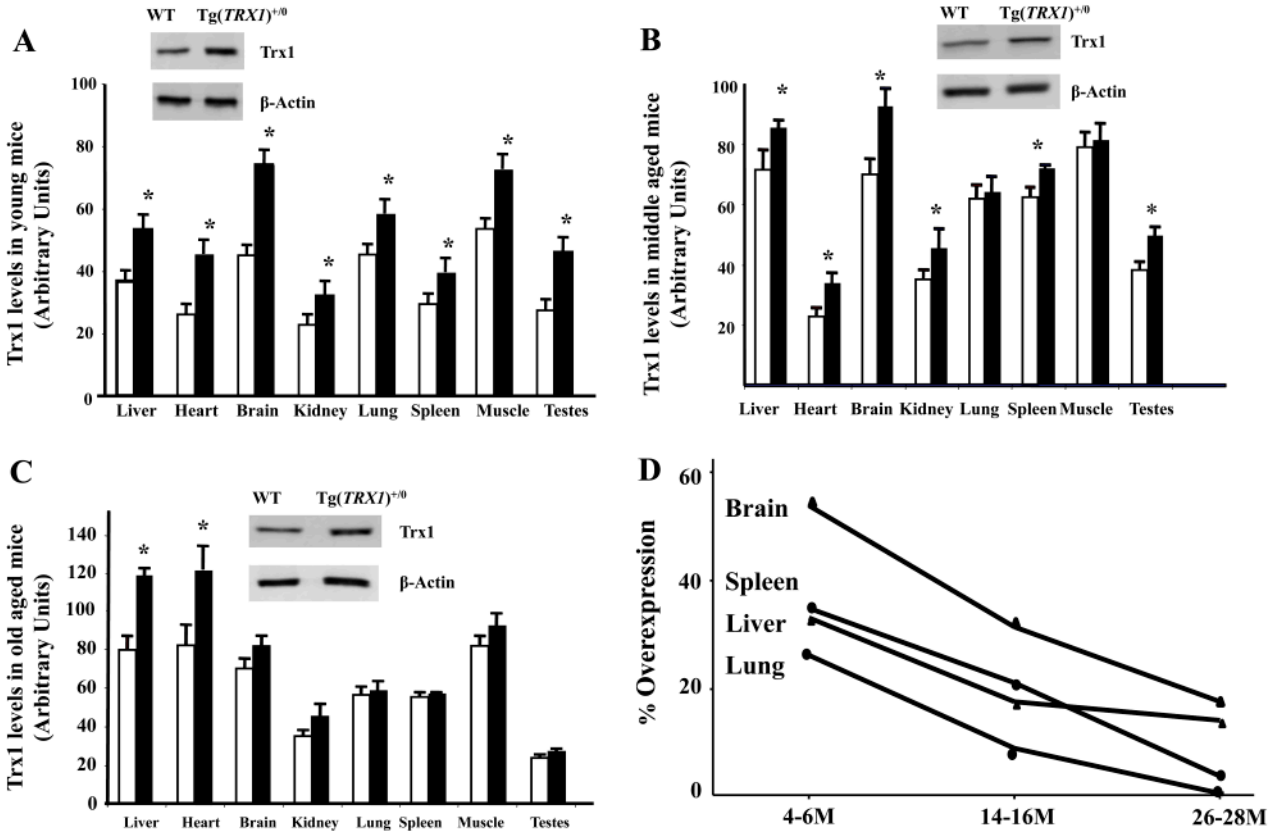

Figure 1. Overexpression of Trx1 in Tg(*TRX1*)$^{+/0}$ mice. The levels of Trx1 protein were determined by Western blot in various tissues of young (4–6 months old [Graph A: left, top]), middle (14–16 months old [Graph B: right, top]), and old (26–28 months old [Graph C: left, bottom]) aged Tg(*TRX1*)$^{+/0}$ (closed bars) and wild-type (WT) mice (open bars). The data are the mean ± *SEM* from three to five mice. Trx1 was significantly higher (*) in the tissues of the Tg(*TRX1*)$^{+/0}$ mice compared with WT mice ($p < .05$). Western blots for liver samples from each age group are shown with their respective graphs. Graph D (right, bottom) gives the percent overexpression of Trx1 in the lung, liver, spleen, and brain of Tg(*TRX1*)$^{+/0}$ mice compared with WT mice at the three ages studied. These data were obtained from Graphs A, B, and C.

error of the mean and were analyzed by the nonparametric test of analysis of the variance. All pair-wise contrasts were computed using Tukey error protection at 95% confidence interval, unless otherwise indicated. Differences were considered statistically significant at $p < .05$.

Results

Overexpression of Trx1 in Tissues From Tg(TRX1)$^{+/0}$ Mice

The levels of Trx1 in tissues from young (4–6 months old), middle (14–16 months old), and old (26–28 months old) Tg(*TRX1*)$^{+/0}$ and WT mice were measured using Western blot analysis. The Trx1 protein levels were significantly higher (29%–54%) in all the 8 tissues we examined in the young Tg(*TRX1*)$^{+/0}$ mice compared with their WT littermates (Figure 1A). The biological activity of Trx was significantly higher in the young Tg(*TRX1*)$^{+/0}$ mice compared with their WT littermates (data not shown). However, the levels of Trx1 overexpression decreased in the middle and old age groups (Figure 1B and C). Figure 1D shows age-related decrease of levels of Trx1 overexpression in the lung, liver, spleen, and brain.

Redox Status of Trx1 and GSH in Livers

Because Trx1, different from other antioxidant enzymes, plays major roles in the maintenance of the cellular redox state and in redox signaling regulation (21) and because several reports have mentioned that a disturbance in the redox state of an organism leads to aging and age-related diseases (36–38), we determined if Trx1 overexpression could alter the redox states of GSH and Trx1 in the liver of young mice (4–6 months old). Our results in Figure 2A show that overexpression of Trx1 significantly increased the reduced state of Trx1 in the liver tissue (30%), which was correlated to increased Trx reductase activity (Figure 2B) but did not alter the redox state of GSH in the liver (Figure 3A). Also, we did not observe significant changes in the redox state of free cysteine (CySH/CySS) or of GSH in plasma (Figure 3B and C).

Levels of Trx2, Glutaredoxin, and Glutathione in Tissues From Tg(TRX1)$^{+/0}$ Mice

Because biological functions of Trx2 (mitochondrial form of Trx), glutathione, and glutaredoxin complement Trx1, it was important to determine if the levels of Trx2, glutaredoxin, and glutathione were altered in response to

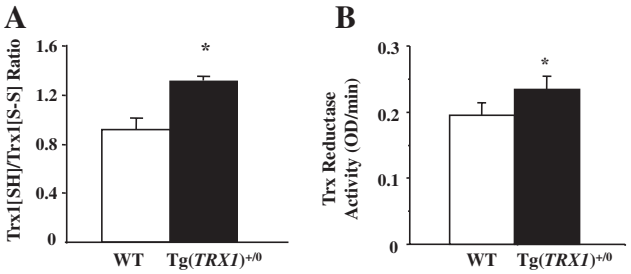

Figure 2. Redox state of Trx1 and Trx Reductase activity in Tg(*TRX1*)$^{+/0}$ mice. The redox state of Trx1 (Graph A: left) was measured in liver cytosolic fractions from young (4–6 months old) Tg(*TRX1*)$^{+/0}$ and wild-type (WT) mice by Redox Western blot using AMS as the alkylating agent. The redox state of Trx1 in the liver was significantly increased (30%) in Tg(*TRX1*)$^{+/0}$ mice (closed bar) compared with WT mice (open bar). The activity of Trx reductase (Graph B: right) was measured in liver from young (4–6 months old) Tg(*TRX1*)$^{+/0}$ and WT mice. Trx reductase activity showed a significant increase in the liver of Tg(*TRX1*)$^{+/0}$ mice (closed bar) compared with WT mice (open bar). The data are the mean of six animals ± *SEM*; the asterisk denotes those values that are significantly different from WT mice at the $p \leq .05$ level.

increased Trx levels. The data in Figure 4 show that no significant changes in Trx2 (Figure 4A) and glutaredoxin (Figure 4B) levels were observed in the liver of young (4–6 months old) Tg(*TRX1*)$^{+/0}$ and WT control mice. Total glutathione levels in liver were slightly higher in the young (4–6 months old) Tg(*TRX1*)$^{+/0}$ mice compared with the WT control (Figure 5), which is consistent with the observation that overexpression of Trx enhances cysteine uptake, resulting in higher glutathione levels in the cells (39). The young (4–6 months old) Tg(*TRX1*)$^{+/0}$ and WT control mice showed similar glutathione levels in the kidney and brain. Therefore, the data in Figures 4 and 5 show that the overexpression of Trx1 in the Tg(*TRX1*)$^{+/0}$ mice was not associated with downregulation of Trx2, glutaredoxin, and total glutathione levels.

Major Antioxidant Enzyme Activities in Tissues From Tg(TRX1)$^{+/0}$ Mice

The activities of the other major antioxidant enzymes were also measured in the Tg(*TRX1*)$^{+/0}$ and WT mice because it is possible that an increase in Trx activity could initiate a compensatory reduction in the activities of other components of the antioxidant system. The data in Figure 6 show that the activities of Cu/ZnSOD, MnSOD, catalase, and GPX were similar in the tissues from the young (4–6 months old) Tg(*TRX1*)$^{+/0}$ and WT mice. Thus, the data in Figure 6 show that Trx1 overexpression in the tissues of the Tg(*TRX1*)$^{+/0}$ mice did not downregulate the major antioxidant defense system.

Levels of Protein Carbonyls and Disulfides Bonds in Tissues From Tg(TRX1)$^{+/0}$ Mice

Because Trx is directly involved in the reduction of disulfides in proteins (40), we examined whether increased levels of Trx1 had any effect on the amount of disulfide bonds in proteins. The disulfide bonds in proteins were measured, using the disulfide detection assay described by Chaudhuri and colleagues (29), and the data are shown in Figure 7A. The protein extracts of liver from young (4–6 months old) Tg(*TRX1*)$^{+/0}$ mice showed a significantly reduced level (34% less) of disulfides in the protein compared with WT control mice, indicating that the Tg(*TRX1*)$^{+/0}$ mice have more reduced proteins in liver in vivo.

The levels of protein carbonyls in liver of the Tg(*TRX1*)$^{+/0}$ mice (Figure 7B) were also measured because the presence of protein carbonyls is a good indicator of protein oxidation (28). The protein carbonyl levels were significantly less (53%) in the livers of young (4–6 months old) Tg(*TRX1*)$^{+/0}$ mice compared with WT mice. Thus, the data, shown in Figure 7, suggest that the overexpression of Trx1 reduced the oxidative damage to the proteins in vivo. Interestingly, we found that the reduction in Trx1 expression with age directly correlates with reduced protection against protein carbonylation, for example, the protein carbonyl levels in young (4–6 months old) Tg(*TRX1*)$^{+/0}$ mice were approximately 50% lower than those of young WT mice (Figure 7B); however, a reduction of only 14% in protein carbonyls was found in old (26–28 months old) Tg(*TRX1*)$^{+/0}$ compared with old WT mice (Figure 7C).

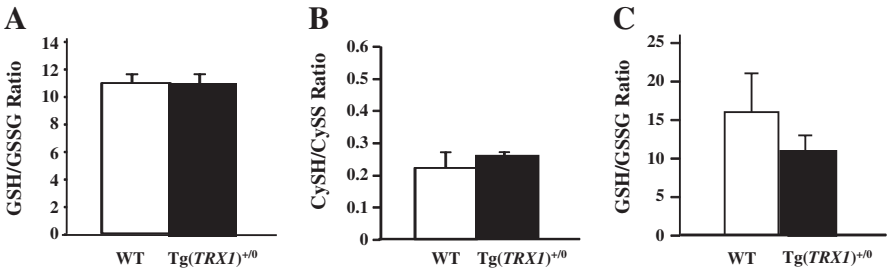

Figure 3. Redox states of GSH and free cysteine in Tg(*TRX1*)$^{+/0}$ mice. GSH in liver (Graph A: left) and free cysteine (CySH/CySS [Graph B: middle]) and GSH (Graph C: right) in plasma of young mice (4–6 months old) were measured using N-dansyl derivatives and high-performance liquid chromatography with fluorescence detection. The redox state of GSH was similar in the liver from Tg(*TRX1*)$^{+/0}$ mice (closed bar) and wild-type mice (open bar). No significant changes were observed in the redox state of free cysteine (CySH/CySS) or of GSH in plasma. The data are the mean of six animals ± *SEM*.

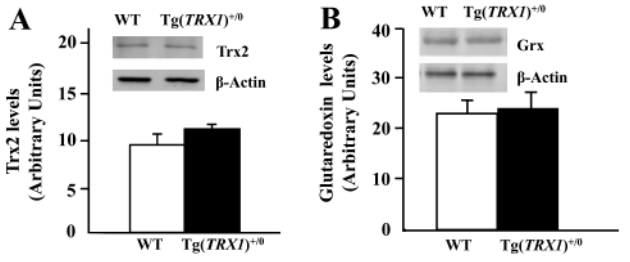

Figure 4. Levels of Trx2 and glutaredoxin in the tissues of Tg(*TRX1*)$^{+/0}$ and wild-type (WT) mice. The levels of Trx2 (Graph A: left) and glutaredoxin (Graph B: right) were measured in liver from young (4–6 months old) Tg(*TRX1*)$^{+/0}$ mice (closed bar) and WT mice (open bar) by Western blot. Western blots are shown with their respective graphs. No significant difference was observed in Trx2 or glutaredoxin levels in the liver of Tg(*TRX1*)$^{+/0}$ mice compared with WT mice. The data in Graphs A and B are the mean ± *SEM* from three to five mice.

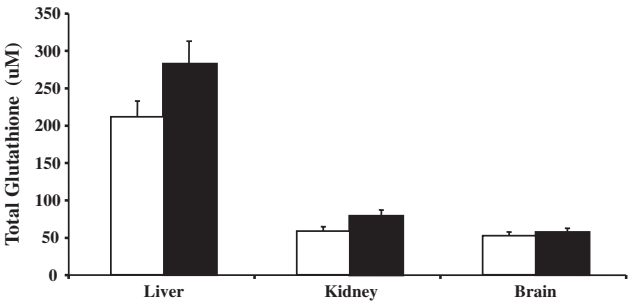

Figure 5. Levels of total glutathione in the tissues of Tg(*TRX1*)$^{+/0}$ and wild-type (WT) mice. The levels of total glutathione were measured in liver, kidney, and brain homogenates from young mice (4–6 months old). The data in the Graphs are the mean ± *SEM* from three mice. The levels of total glutathione levels in liver were slightly higher in the Tg(*TRX1*)$^{+/0}$ mice (closed bar) compared with WT mice (open bar). The levels of total glutathione levels in kidney and brain were similar in Tg(*TRX1*)$^{+/0}$ and WT mice.

Lipid Peroxidation (F2-isoprostane levels) and DNA Oxidation (8-oxodG levels)

Then we tested whether Trx1 overexpression protects against oxidative damage by measuring levels of lipid peroxidation (F_2 isoprostanes) in serum and DNA oxidation (8-oxodG) in liver from old (26–28 months) Tg(*TRX1*)$^{+/0}$ and WT mice. Levels of F_2-isoprostanes (22%, Figure 8A) were significantly lower in the Tg(*TRX1*)$^{+/0}$ mice compared with WT mice, which could indicate that whole-body oxidative stress is lower in the Tg(*TRX1*)$^{+/0}$ mice compared with WT

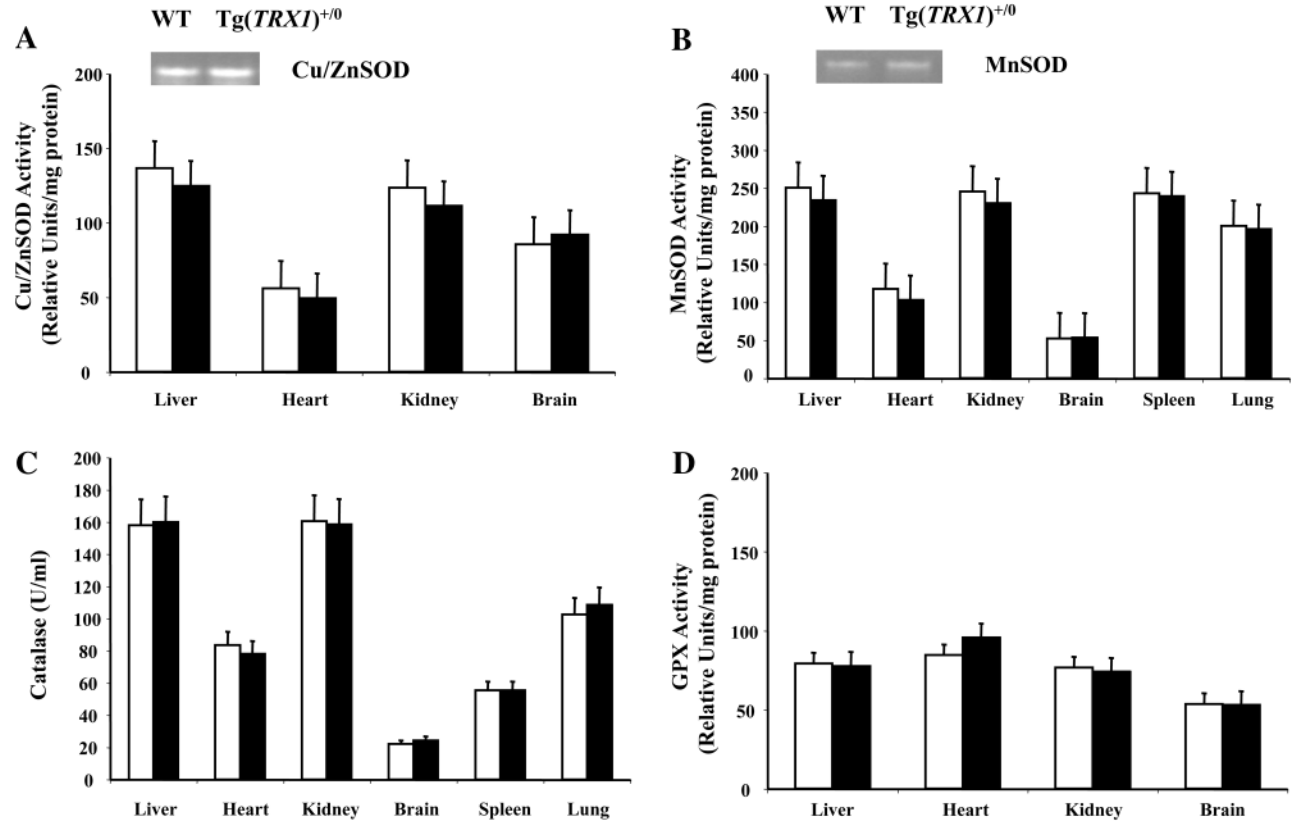

Figure 6. Cu/ZnSOD, MnSOD, catalase, and GPX activity in tissues of the Tg(*TRX1*)$^{+/0}$ mice. The activities of Cu/ZnSOD (Graph A: left, top), MnSOD (Graph B: right, top), catalase (Graph C: left, bottom), and GPX (Graph D: right, bottom) were measured in tissue extracts from young mice (4–6 months old). Cu/ZnSOD and MnSOD activity gels are shown with their respective graphs. Data are the mean ± *SEM* of three Tg(*TRX1*)$^{+/0}$ and three wild-type (WT) mice. The activities of Cu/Zn-SOD, MnSOD, catalase, and GPX were similar between Tg(*TRX1*)$^{+/0}$ (closed bar) and WT mice (open bar).

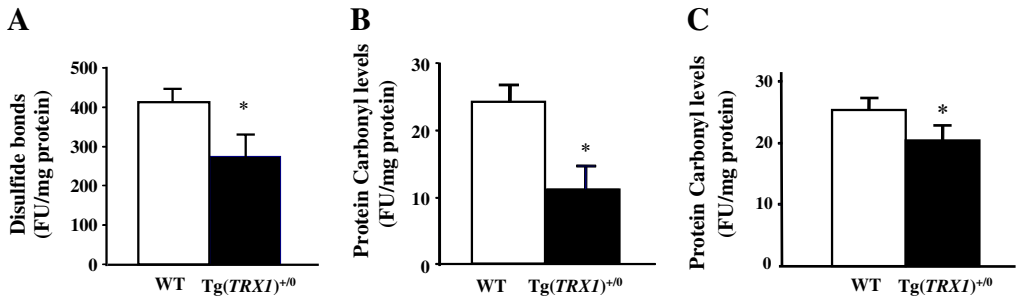

Figure 7. Protein oxidation in the liver of Tg(*TRX1*)$^{+/0}$ and wild-type (WT) mice. The levels of disulfide bonds (Graph A: left) in the liver were measured by a disulfide detection assay. The levels of protein carbonyls were measured using a fluorescence-based method in 4–6 months old (Graph B: middle) and 26–28 months old (Graph C: right) Tg(*TRX1*)$^{+/0}$ mice (closed bar) and WT mice (open bar). The data in Graphs A, B, and C are the mean ± *SEM* from three to five mice, and the data that are significantly lower ($p < .05$) in the Tg(*TRX1*)$^{+/0}$ mice compared with WT mice are indicated by asterisk (*).

mice. However, levels of DNA oxidation were similar between old (26–28 months) Tg(*TRX1*)$^{+/0}$ and WT mice (Figure 8B).

Sensitivity of Tg(TRX1)$^{+/0}$ Mice to Diquat

We compared the responses of young (4–6 months old) Tg(*TRX1*)$^{+/0}$ and WT mice to diquat treatment because diquat has been used to study the protective role of antioxidant enzymes against oxidative stress in mice (41). Plasma levels of ALT activity were measured as a marker of liver damage after a low dose (50 mg/kg) of diquat injection (Figure 9A). In untreated mice, no difference in plasma ALT levels was observed between Tg(*TRX1*)$^{+/0}$ mice and WT mice. Diquat injection resulted in a significant increase in plasma ALT levels in WT and Tg(*TRX1*)$^{+/0}$ mice compared with untreated mice. The Tg(*TRX1*)$^{+/0}$ mice showed significantly lower levels of plasma ALT compared with WT mice after diquat injection, which indicates that the Tg(*TRX1*)$^{+/0}$ mice had less liver damage (ie, decrease in plasma ALT levels) in response to diquat treatment than the WT mice. To correlate the liver damage to oxidative stress, we also measured the levels of protein carbonyls in the livers of the diquat-treated mice. As shown in Figure 9B, the Tg(*TRX1*)$^{+/0}$ mice showed lower amounts of protein carbonyls in liver after diquat treatment.

Another group of young (4–6 months old) mice was injected with diquat at a higher dose (60 mg/kg), and survival curves were compared. As shown in Figure 9C, approximately 90% of the WT mice died within 3 days after the diquat administration; however, only about 50% of the Tg(*TRX1*)$^{+/0}$ mice were dead after the same elapsed time. Therefore, the Tg(*TRX1*)$^{+/0}$ mice showed increased resistance to oxidative stress by diquat injection.

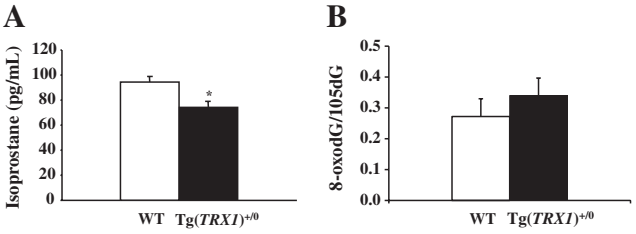

Figure 8. Levels of F_2-isoprostanes in the serum and DNA oxidation in the liver of Tg(*TRX1*)$^{+/0}$ and wild-type (WT) mice. Serum from Tg(*TRX1*)$^{+/0}$ (closed bar) and WT (open bar) mice were processed, and F_2-isoprostanes levels were measured at 26–28 months of age. The F_2-isoprostanes levels in the serum from Tg(*TRX1*)$^{+/0}$ mice were approximately 20% lower compared with age-matched WT control (Graph A: left). The data are obtained from the serum of nine mice per group. Levels of DNA oxidation in the liver of Tg(*TRX1*)$^{+/0}$ (closed bar) and WT (open bar) mice at 26–28 months of age showed no significant difference (Graph B: right).

ASK1 Levels and NFκB Target Genes Expression

We have chosen to study NFκB and ASK1 because these transcription factors/signaling molecules have been shown to be redox sensitive and to be affected by Trx. More importantly, these transcription factors/signaling molecules could play important roles in aging and/or some age-related diseases, for example, cancer, inflammation. Figure 10 shows levels of ASK1/Trx1 complex and phosphorylated JNK. Levels of ASK1/Trx1 complex were significantly higher in young (4–6 months old) Tg(*TRX1*)$^{+/0}$ compared with WT mice (Figure 10A). Levels of phosphorylated JNK were significantly lower in young (4–6 months old) Tg(*TRX1*)$^{+/0}$ compared with WT mice (Figure 10B). We also measured messenger RNA levels of some of the NFkB target genes with qRT-PCR (Figure 10C). Levels of IL-1β messenger RNA were significantly lower in the livers of young (4–6 months old) Tg(*TRX1*)$^{+/0}$ mice compared with WT mice, although levels of CCL5 (chemokine ligand 5) and TNF-α messenger RNA were similar between Tg(*TRX1*)$^{+/0}$ and WT mice.

Survival Curves and End-of-Life Pathology

Survival curves of Tg(*TRX1*)$^{+/0}$ and WT mice from two cohorts are presented in Figure 11. The first cohort consists of 48 male WT and 41 male Tg(*TRX1*)$^{+/0}$ mice (Figure 11A), and the second cohort consists 60 male WT and 60 male Tg(*TRX1*)$^{+/0}$ mice (Figure 11B) and 40 female WT and 40

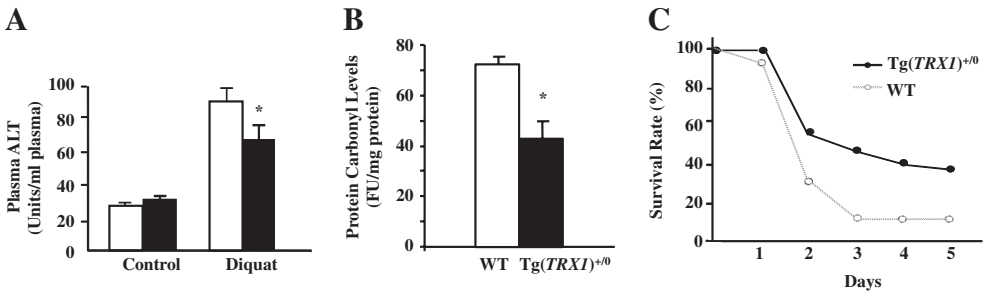

Figure 9. Effect of diquat treatment on hepatotoxicity, protein oxidation, and survival of young (4–6 months old) Tg(*TRX1*)$^{+/0}$ and wild-type (WT) mice. The plasma ALT levels (Graph A: left) were significantly higher ($p < .05$ level) after diquat injection in both Tg(*TRX1*)$^{+/0}$ (closed bar) and WT (open bar) mice compared with untreated groups (*). The Tg(*TRX1*)$^{+/0}$ mice (closed bar) showed significantly lower plasma ALT levels than WT mice (open bar) after diquat injection (*). The data for plasma ALT levels are expressed as the mean ± *SEM* from five mice. Protein carbonyl levels of Tg(*TRX1*)$^{+/0}$ and WT mice after 50 mg/kg diquat injection are shown in Graph B (middle). The data for protein carbonyl levels are expressed as the mean ± *SEM* from five mice. The Tg(*TRX1*)$^{+/0}$ mice showed significantly lower protein carbonyl levels than WT mice after diquat injection. Survival curves of Tg(*TRX1*)$^{+/0}$ and WT mice after the intraperitoneal injection of 60 mg/kg body weight diquat are shown in Graph C (right). Tg(*TRX1*)$^{+/0}$ mice had increased resistance to oxidative stress compared with WT mice. Approximately 6.6% of the WT mice were viable 3 days after diquat injection, whereas 50% of the Tg(*TRX1*)$^{+/0}$ mice were viable.

female Tg(*TRX1*)$^{+/0}$ mice (Figure 11C). The body weights, organ weights, and food consumption were similar between Tg(*TRX1*)$^{+/0}$ and WT mice.

The survival curves of WT mice are similar to the C57BL/6 mice in our aging colony, except that the WT mice showed slightly higher death rate in the earlier part of life. The survival curves were not significantly different between Tg(*TRX1*)$^{+/0}$ and WT mice. Mean; median; 90th, 75th, 25th, and 10th percentile (when 10%, 25%, 75%, or 90% of the mice died); and maximum survivals for each group are presented in Table 1. The male Tg(*TRX1*)$^{+/0}$ mice showed significant increases in 90% survival (both cohorts), and only the first male cohort showed a significant increase in 75% survival compared with WT mice. However, we found no difference in the median, 25%, and 10% survival between Tg(*TRX1*)$^{+/0}$ and WT mice in two male cohorts. In females, although the Tg(*TRX1*)$^{+/0}$ mice seemed to extend life span in the earlier part of life compared with WT mice, none of the survival parameters were statistically significant.

The end-of-life pathological data of the Tg(*TRX1*)$^{+/0}$ and WT mice are presented in Table 2. The major cause of death in these mice was neoplastic disease, especially lymphoma, which is consistent with the end-of-life pathology data from C57BL/6 mice (35). The incidence of fatal tumors was slightly higher in the Tg(*TRX1*)$^{+/0}$ compared with WT mice. On the other hand, the total incidence (both fatal and incidental) of acidophilic macrophage pneumonia, which is one of the common nonneoplastic lesions in C57BL/6 mice, was significantly less in Tg(*TRX1*)$^{+/0}$ compared with WT mice (data not shown).

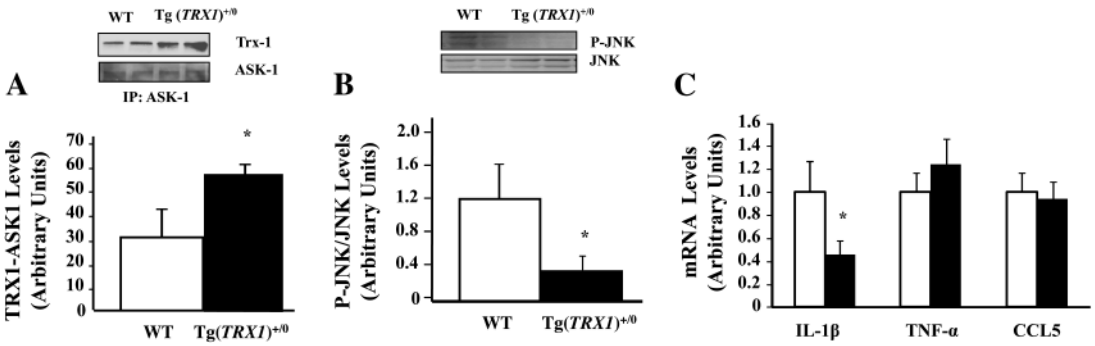

Figure 10. Levels of ASK1/Trx1 complex, JNK phosphorylation, and inflammatory gene expression in Tg(*TRX1*)$^{+/0}$ and wild-type (WT) mice. Levels of ASK1/Trx1 complex and phosphorylated JNK were measured by Western blot analysis in cytosolic liver fractions from young mice (4–6 months old). Western blots for ASK1/Trx1 complex and phosphorylated JNK are shown with their respective graphs. The expression of inflammatory genes was measured by the levels of interleukin (IL)-1β, CCL5, and tumor necrosis factor (TNF) α using quantitative real-time polymerase chain reaction. Levels of ASK1/Trx1 complex were significantly higher in Tg(*TRX1*)$^{+/0}$ compared with WT mice (Graph A: left). Levels of phosphorylated JNK were significantly lower in Tg(*TRX1*)$^{+/0}$ compared with WT mice (Graph B: middle). Levels of IL-1β messenger RNA (mRNA) were significantly lower in the livers from young (4–6 months old) Tg(*TRX1*)$^{+/0}$ mice compared with WT mice (Graph C: right). Levels of CCL5 (chemokine) and TNF-α mRNA were similar in the livers from young (4–6 months old) Tg(*TRX1*)$^{+/0}$ and WT mice. The data are the mean of three to five animals ± *SEM*. The asterisk denotes those values that are significantly different from WT mice at the $p \leq .05$ level.

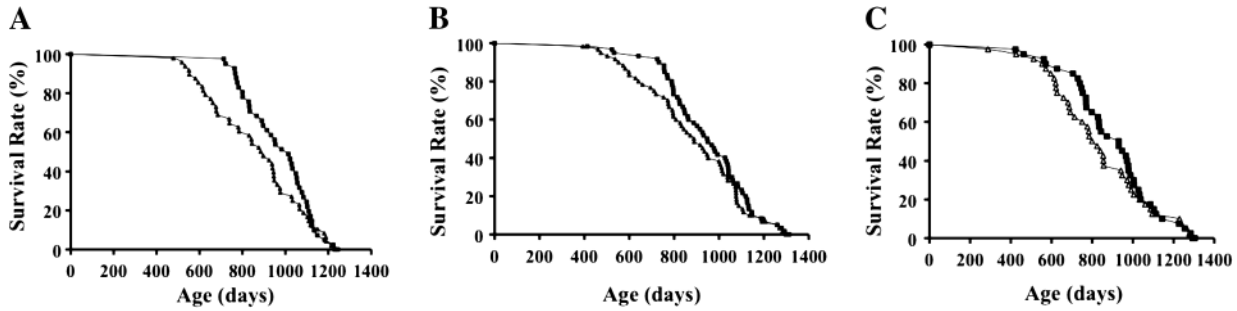

Figure 11. The survival curves of Tg(*TRX1*)$^{+/0}$ and wild-type (WT) mice. Survival curves of Tg(*TRX1*)$^{+/0}$ and WT mice from two cohorts are presented. The first cohort consists of 48 male WT and 41 male Tg(*TRX1*)$^{+/0}$ mice (Graph A: left), and the second cohort consists 60 male WT and 60 male Tg(*TRX1*)$^{+/0}$ mice (Graph B: middle) and 40 female WT and 40 female Tg(*TRX1*)$^{+/0}$ mice (Graph C: right). The survival curves were compared statistically using the log-rank test. The survival curves were not significantly different between Tg(*TRX1*)$^{+/0}$ and WT mice. The male Tg(*TRX1*)$^{+/0}$ mice showed significant increases in 90% survival (both cohorts), and only the first male cohort showed a significant increase in 75% survival compared with WT mice. However, we found no difference in the median, 25%, and 10% survival between Tg(*TRX1*)$^{+/0}$ and WT mice in two male cohorts. In females, although the Tg(*TRX1*)$^{+/0}$ mice seemed to extend life span in the earlier part of life compared with WT mice, none of the survivals parameters were statistically significant.

Discussion

Over the past three decades, the *Oxidative Stress Theory of Aging* has been extensively studied. Several lines of evidence support the oxidative stress theory of aging. First, the levels of oxidative damage to lipid, DNA, and protein have been reported to increase with age in a variety of tissues and animal models (42). Second, many long-lived animals show reduced oxidative damage and/or increased resistance to oxidative stress (42–47). However, all the experimental manipulations that increase life span also alter processes other than oxidative stress/damage; therefore, the increase in longevity in these animal models could arise through another mechanism(s). Recent data from Buffenstein's laboratory show that naked mole rats, which have a life span approaching 30 years, have increased oxidative damage compared with the short-lived mouse (48). This observation calls into question the role of oxidative damage in aging.

Transgenic/knockout animals provide investigators with a unique system for studying the underlying mechanisms of various biological processes. To test the oxidative stress theory of aging, several groups have genetically altered various components of the antioxidant defense system in mice and studied the effect of these alterations on life span. However, many of the studies with transgenic mice that overexpress various antioxidant enzymes did not show extension of life span compared with the WT controls, although the overexpression of antioxidant enzymes was associated with increased resistance to oxidative stress and/or reduced oxidative damage. On the other hand, transgenic mice that overexpress catalase in mitochondria showed an increase in life span, which was associated with reduced oxidative damage (49). Therefore, overexpression of antioxidant enzymes does not appear to increase the life span of mice, except for the study by Schriner and colleagues (49).

There is also considerable information on the effect of underexpressing antioxidant enzymes on aging. Our group has studied the effect of reduced expression of MnSOD on aging and pathology using mice heterozygous for the *Sod2* gene (*Sod2*$^{+/-}$ mice). The *Sod2*$^{+/-}$ mice showed higher levels of DNA oxidation and a higher incidence of cancer; however, there was no difference in the life span between the *Sod2*$^{+/-}$ and WT mice (50). Cu/ZnSOD null mice, which lack Cu/ZnSOD, are shown to have a shorter life span compared with the WT control mice (51). However, the short life span of these knockout mice (in the C57BL/6 background) appears to be due to a high incidence (approximately 90%) of hepatocellular carcinoma, which is extremely rare in

Table 1. Survival Data of Tg(*TRX1*)$^{+/0}$ Mice (days)

	First Cohort		Second Cohort			
	Male		Male		Female	
	WT	Tg(*TRX1*)$^{+/0}$	WT	Tg(*TRX1*)$^{+/0}$	WT	Tg(*TRX1*)$^{+/0}$
Mean	866	972	881	943	835	899
90%	572	771*	571	753*	570	621
75%	673	832*	717	797	651	765
50%	891	1,014	889	949	812	930
25%	1,041	1,099	1,074	1,088	994	1,028
10%	1,159	1,134	1,143	1,151	1,230	1,152

Note: WT = wild type.
*$p < .05$.

Table 2. End-of-Life Pathology of Tg(*TRX1*)$^{+/0}$ Mice

	WT	Tg(*TRX1*)$^{+/0}$
Neoplasm	25 (58.1%)	30 (73.2%)
Lymphoma	20 (46.5%)	26 (63.4%)
Hemangioma	2	2
Others	3	2
Nonneoplasm	18 (41.9%)	11 (26.8%)
Glomerulonephritis	8	6
Others	10	5
Total	43	41

Note: WT = wild type.

WT mice in the C57BL/6 genetic background (35,52). Our recent studies demonstrated that the survival curves of the mice that were deficient in Gpx1 and MnSOD (*Gpx1*$^{-/-}$, *Sod2*$^{+/-}$, *Gpx1*$^{+/-}$ × *Sod2*$^{+/-}$, and *Gpx1*$^{-/-}$ × *Sod2*$^{+/-}$) are essentially the same as WT mice. These data are also inconsistent with the oxidative stress theory of aging.

Therefore, the studies using both transgenic and knockout mouse models showed that alterations in the antioxidant defense system do not affect life span in spite of the alterations in resistance to oxidative stress and oxidative damage to macromolecules, which brings into question the role of oxidative damage in aging (53).

In 1999, Yodoi and colleagues generated transgenic mice overexpressing Trx1 with a transgene containing the human TRX1 cDNA fused to the β-actin promoter (11). Their survival study (19,20) indicated that the Tg(*TRX1*)$^{+/0}$ mice had an extended longevity compared with the WT mice. Their survival results are very exciting because (a) these mice are the second mouse model (the first one is mCAT mice) supporting the oxidative stress theory of aging and (b) these data could indicate the importance of redox state maintenance during aging. In addition to its antioxidant property, Trx1, unlike other antioxidant enzymes, plays major roles in the maintenance of the cellular redox state and in redox signaling regulation (21). Several reports have mentioned that a disturbance in the redox state of an organism leads to aging and age-related diseases (36–38). However, this survival study has several possible deficits. First, because this survival study was conducted under conventional housing conditions, the infectious status of these mice potentially changed their normal aging process. Second, the life span of the WT C57BL/6 mice in their colony was shorter than the C57BL/6 mice raised under barrier conditions (eg, the median life span was approximately 23 months of age, which is much shorter than the median life span of C57BL/6 mice in aging colonies at San Antonio [29–30 months of age]). Therefore, we conducted the aging study to examine the effects of increased levels of Trx1 on oxidative stress in vivo and its long-term pathophysiological consequences under optimal housing conditions using a unique animal model overexpressing Trx1.

We found that the levels of Trx1 were significantly higher in all the tissues examined in the young Tg(*TRX1*)$^{+/0}$ mice compared with the WT control. The levels of Trx1 were 29%–54% higher in all the eight tissues examined, which was associated with similar levels of increase in biological activity of Trx in the Tg(*TRX1*)$^{+/0}$ mice compared with the WT control. Overexpression of Trx1 was significantly associated with a reduced state of Trx1 in the liver tissue (30%) mainly due to increased Trx1 reductase activities. However, it did not alter the redox state of GSH in liver, free cysteine (CySH/CySS), or GSH in plasma. The increased levels of Trx1 caused no compensatory downregulation in Trx2, glutaredoxin, glutathione, and other major antioxidant enzymes.

As expected, the increased levels of Trx1 provided more resistance to oxidative stress in vivo. The levels of carbonyl and disulfide bonds in the protein in the tissues of young Tg(*TRX1*)$^{+/0}$ mice were significantly lower compared with the WT control, which indicates that the overexpression of Trx1 reduced the levels of oxidized protein in vivo under normal physiological conditions. To further explore the protective roles of Trx1 against endogenous oxidative stress, we also tested the sensitivity to induced oxidative stress by diquat treatment. The young Tg(*TRX1*)$^{+/0}$ mice showed higher survival after diquat injection compared with WT mice. This higher survival of the Tg(*TRX1*)$^{+/0}$ mice was associated with less liver injury assessed by plasma alanine aminotransferase (ALT) levels, which is commonly used to monitor liver injury, and lower levels of oxidative damage to protein. Therefore, our results demonstrated that overexpression of Trx1 increased resistance to oxidative stress in vivo, via its protective role against oxidative damage to proteins, which is consistent with a previous study with ischemic injury in brain (11). In old animals, levels of protein carbonylation and lipid peroxidation in Tg(*TRX1*)$^{+/0}$ mice were significantly lower compared with the WT control, but levels of DNA oxidation measured by oxo8dG were similar between Tg(*TRX1*)$^{+/0}$ and WT mice.

Our initial survival study showed that male Tg(*TRX1*)$^{+/0}$ mice demonstrated a significantly extended earlier part of life span but no change in maximum life span. To further confirm our initial observation, we conducted another survival study with males and females. Again, male Tg(*TRX1*)$^{+/0}$ mice showed a significant increase in 90% survival, but no significant life extension was observed in median and maximum life spans. In female mice, no significant change in life span was observed, although they showed a slight extension of 75% survival compared with the WT control. These survival data agree in part with the previous study by Yodoi and colleagues, who showed that overexpression of Trx1 significantly increases median and maximum life spans (19,20). The different results between this and previous studies could be due to the difference in the housing conditions of the mouse colony used. The previous study showed a maximum longevity of approximately 32 months (20), whereas the mice in our colony lived about 20% longer (40 months) than those maintained under conventional

housing conditions. Therefore, our survival data did show that the overexpression of Trx1 increased the earlier part of life span (at least 75% survival in males), but no extension was observed in the maximum life span. These results led us to the following questions: (a) Why did Trx1 overexpression show some beneficial effects on life span, although most of the other antioxidants overexpression failed to extend life span and (b) Why did Trx1 overexpression show extension of life span only in the earlier part of life?

Several studies demonstrated that the cellular redox state plays an important role in physiological responses to oxidative stress and aging. Because these data are based on measurements of the glutathione redox state (54–56), it is very interesting to test if the changes to the Trx1 redox state could affect aging. Our data demonstrated that the life-span extension in the earlier life of Tg(*TRX1*)$^{+/0}$ mice is correlated to increased levels of the Trx1 redox state. This enhanced Trx1 redox state could play an important role in an organism's ability to better respond to oxidative stress by inhibiting signaling pathways that are dependent on the cellular redox state. Because Tg(*TRX1*)$^{+/0}$ mice showed less incidence of acidophilic macrophage pneumonia and substantial evidence suggest the important role of inflammation on aging, we measured the representative target genes in the NFκB pathway by qRT-PCR, that is, IL-1β, CCL5 (chemokine), and TNF-α. The messenger RNA levels of IL-1β were significantly lower in the liver from Tg(*TRX1*)$^{+/0}$ mice compared with WT mice. Because IL-1β could be involved in the widespread systemic inflammatory process that may play important roles in aging, reduction in systemic inflammation including in the lung could be one of the contributing factors for the extension of life span in the earlier part of life in the Tg(*TRX1*)$^{+/0}$ mice.

The next question is why Trx1 overexpression showed an extension of life span only in the earlier part of life. A possible explanation is that overexpression of Trx 1 decreased with age in most of the tissues in the Tg(*TRX1*)$^{+/0}$ mice. These mice were generated with the β-actin promoter to drive the expression of the transgene. Age-related decrease in overexpression of the transgene has been also observed by other investigators (Drs. J. Nelson from the University of Texas Health Science Center at San Antonio and D. Jones from Emory University for Hsp70 cDNA and Trx2 cDNA, respectively, who have used the β-actin promoter [personal communications]). The beneficial effects of Trx1 could be diminished due to the reduced levels of overexpression during aging, which was correlated with less reduction in protein carbonylation levels. Another possible explanation is that Trx1 could be involved in tumor growth in the old animals because of its antiapoptotic effect by the inhibition of the ASK-1 pathway (57–59). Our data showed that Tg(*TRX1*)$^{+/0}$ mice had higher levels of the ASK1/Trx1 complex and reduced JNK activation. The end-of-life pathology data showed that Tg(*TRX1*)$^{+/0}$ mice had a slightly higher incidence of fatal tumors compared with WT mice. This may not be a surprising observation because Trx1 is overexpressed in various cancers (16,60,61). Because apoptosis plays important roles in carcinogenesis, overexpression of Trx1 could be involved in cancer growth by its antiapoptotic action in old mice. However, the possible role and mechanisms of Trx1 overexpression in spontaneous tumor development remain to be further examined in different strain and species because, unlike humans, C57BL/6 mice have a very high incidence of cancer and lymphoma (35).

Our study demonstrated that overexpression of Trx1 in mice increased resistance to oxidative stress and reduced oxidative damage in vivo. Changes in the redox sensitive signaling pathway have also been seen, possibly due to the changes in the redox state in the cells. Increased resistance to oxidative stress and reduced inflammation could be the contributing factors extending the life span compared with WT mice in the earlier part of life. On the other hand, overexpression of Trx1 in mice showed little benefits on maximum life span probably due to the age-related decline of overexpression of Trx1. Although our observation is very exciting, it has not been determined if Trx1 overexpression has beneficial effects on health span and age-related functional changes in various organs; these studies need to be conducted in the future. The exact role of Trx1 in health and aging also needs to be further examined in other species, including humans.

Funding

This research was supported by VA Merit Review Grant from the Department of Veteran Affairs (Y.I.), National Institutes of Health Grant AG13319 (Y.I.), The American Federation for Aging Research grant (Y.I.), and Grant from Glenn Foundation (Y.I.).

References

1. Tagaya Y, Maeda Y, Mitsui A, et al. ATL-derived factor (ADF), an IL-2 receptor/Tac inducer homologous to thioredoxin; possible involvement of dithiol-reduction in the IL-2 receptor induction. *EMBO J*. 1989;8:757–764.
2. Spyrou G, Enmark E, Miranda-Vizuete A, Gustafsson JA. Cloning and expression of a novel mammalian thioredoxin. *J Biol Chem*. 1997;272:2936–2941.
3. Matsui M, Oshima M, Oshima H, Takaku K, Maruyama T, Yodoi J. Early embryonic lethality caused by targeted disruption of the mouse thioredoxin gene. *Dev Biol*. 1996;178:179–185.
4. Nonn L, Williams RR, Erickson RP, Powis G. The absence of mitochondrial thioredoxin 2 causes massive apoptosis, exencephaly, and embryonic lethality in homozygous mice. *Mol Cell Biol*. 2003;23:916–922.
5. Chae HZ, Kim HJ, Kang SW, Rhee SG. Characterization of three isoforms of mammalian peroxiredoxin that reduce peroxides in the presence of thioredoxin. *Diabetes Res Clin Pract*. 1999;45:101–112.
6. Chae HZ, Kang SW, Rhee SG. Isoforms of mammalian peroxiredoxin that reduce peroxides in presence of thioredoxin. *Methods Enzymol*. 1999;300:219–226.
7. Kim K, Kim IH, Lee KY, Rhee SG, Stadtman ER. The isolation and purification of a specific "protector" protein which inhibits enzyme inactivation by a thiol/Fe(III)/O2 mixed-function oxidation system. *J Biol Chem*. 1988;263:4704–4711.
8. Brot N, Weissbach L, Werth J, Weissbach H. Enzymatic reduction of protein-bound methionine sulfoxide. *Proc Natl Acad Sci USA*. 1981;78:2155–2158.

9. Brot N, Weissbach H. Peptide methionine sulfoxide reductase: biochemistry and physiological role. *Biopolymers*. 2000;55:288–296.
10. Levine RL, Berlett BS, Moskovitz J, Mosoni L, Stadtman ER. Methionine residues may protect proteins from critical oxidative damage. *Mech Ageing Dev*. 1999;107:323–332.
11. Takagi Y, Mitsui A, Nishiyama A, et al. Overexpression of thioredoxin in transgenic mice attenuates focal ischemic brain damage. *Proc Natl Acad Sci USA*. 1999;96:4131–4136.
12. Arnér ESJ, Holmgren A. Physiological functions of thioredoxin and thioredoxin reductase. *Eur J Biochem*. 2000;267:6102–6109.
13. Abate C, Patel L, Rauscher FJ III, Curran T. Redox regulation of Fos and Jun DNA-binding activity in vitro. *Science*. 1990;249: 1157–1161.
14. Galter D, Mihm S, Droge W. Distinct effects of glutathione disulphide on the nuclear transcription factor kB and the activator protein-1. *Eur J Biochem*. 1994;221:639–648.
15. Toledano MB, Leonard WJ. Modulation of transcription factor NF-KB binding activity by oxidation-reduction in vitro. *Proc Natl Acad Sci USA*. 1991;88:4328–4332.
16. Saitoh M, Nishitoh H, Fujii M, et al. Mammalian thioredoxin is a direct inhibitor of apoptosis signal-regulating kinase (ASK) 1. *EMBO J*. 1998;17:2569–2606.
17. Miranda-Vizuete A, Gonzalez J, Gahmon G, Burghoorn J, Placido N, Swoboda P. Lifespan decrease in a Caenorhabditis elegans mutant lacking TRX-1, a thioredoxin expressed in ASJ sensory neurons. *FEBS Lett*. 2006;580:484–490.
18. Svensson MJ, Larsson J. Thioredoxin-2 affects lifespan and oxidative stress in Drosophila. *Hereditas*. 2007;144:25–32.
19. Mitsui A, Hamuro J, Nakamura H, et al. Overexpression of human thioredoxin in transgenic mice controls oxidative stress and life span. *Antioxid Redox Signal*. 2002;4:693.
20. Nakamura H, Mitsui A, Yodoi J. Thioredoxin overexpression in transgenic mice. *Methods Enzymol*. 2002;347:436–440.
21. Holmgren A. Enzymatic reduction-oxidation of protein disulfides by thioredoxin. *Methods Enzymol*. 1984;107:295–300.
22. Ritz D, Beckwith J. Redox state of cytoplasmic thioredoxin. *Methods Enzymol*. 2002;347:360–370.
23. Halvey PJ, Watson WH, Hanszen JM, Go YM, Samali A, Jones DP. Compartmental oxidation of thiol-disulphide redox couples during epidermal growth factor signalling. *Biochem J*. 2005;386:215–219.
24. Jones DP, Carlson JL, Samiec PS, et al. Glutathione measurement in human plasma. Evaluation of sample collection, storage and derivatization condition for analysis of dansyl derivatives by HPLC. *Clin Chim Acta*. 1998;275:175–184.
25. Williams MD, Van Remmen H, Conrad CC, Huang TT, Epstein CJ, Richardson A. Increased oxidative damage is correlated to altered mitochondrial function in heterozygous manganese superoxide dismutase knockout mice. *J Biol Chem*. 1998;273:28510–28515.
26. Sun Y, Elwell JH, Oberley LW. A simultaneous visualization of the antioxidant enzymes glutathione peroxidase and catalase on polyacrylamide gels. *Free Radic Res Commun*. 1988;5:67–75.
27. Beauchamp C, Fridovich I. Superoxide dismutase: improved assays and an assay applicable to acrylamide gels. *Analyt Biochem*. 1971; 44:276–287.
28. Chaudhuri AR, de Waal EM, Pierce A, Van Remmen H, Ward HF, Richardson A. Detection of protein carbonyls in aging liver tissue: a fluorescence-based proteomic approach. *Mech Ageing Dev*. 2006;127: 849–861.
29. Chaudhuri AR, Khan IA, Luduena RF. Detection of disulfide bonds in bovine brain tubulin and their role in protein folding and microtubule assembly in vitro: a novel disulfide detection approach. *Biochemistry*. 2001;40:8834–8841.
30. Morrow JD, Roberts II LJ. The isoprostanes: current knowledge and directions for future research. *Biochem Pharm*. 1996;51:1–9.
31. Hamilton ML, Guo ZM, Fuller CD, et al. A reliable assessment of 8-oxo-2-deoxyguanosine levels in nuclear and mitochondrial DNA using the sodium iodide method to isolate DNA. *Nucleic Acids Res*. 2001;29:2117–2126.
32. Andersen PK, Borgan O, Gill RD, Keiding N. *Statistical Models Based on Counting Processes*; New York: Spring-Verlag; 1993.
33. Wang C, Li Q, Redden DT, Weindruch R, Allison DB. Statistical methods for testing effects on "maximum lifespan". *Mech Ageing Dev*. 2004;125:629–632.
34. Bronson RT, Lipman RD. Reduction in rate of occurrence of age related lesions in dietary restricted laboratory mice. *Growth Dev Aging*. 1991;55:169–184.
35. Ikeno Y, Hubbard GB, Lee S, et al. Housing density does not influence the longevity effect of calorie restriction. *J Gerontol*. 2005;12:1510–1517.
36. Finkel T. Oxidant signals and oxidative stress. *Curr Opin Cell Biol*. 2003;15:247–254.
37. Papaconstantinou J. Unifying model of the programmed (intrinsic) and stochastic (extrinsic) theories of aging. *Ann N Y Acad Sci*. 1994; 719:195–211.
38. Rebrin I, Forster MJ, Sohal RS. Effects of age and caloric restriction on glutathione redox state in mice. *Brain Res*. 2007;1127:10–18.
39. Iwata S, Hori T, Sato N, et al. Adult T cell leukemia (ATL)-derived factor/human thioredoxin prevents apoptosis of lymphoid cells induced by L-cystine and glutathione depletion: possible involvement of thiol-mediated redox regulation in apoptosis caused by pro-oxidant state. *J Immunol*. 1997;158:3108–3117.
40. Holmgren A. Thioredoxin. *Annu Rev Biochem*. 1985;54:237–271.
41. Fu Y, Cheng W, Porres JM, Ross DA, Lei XG. Knockout of cellular glutathione peroxidase gene renders mice susceptible to diquat-induced oxidative stress. *Free Radic Bio Med*. 1999;27:605–611.
42. Bokov A, Chaudhuri A, Richardson A. The role of oxidative damage and stress in aging. *Mech Ageing Dev*. 2004;125:811–826.
43. Sohal RS, Weindruch R. Oxidative stress, caloric restriction, and aging. *Science*. 1996;273:59–63.
44. Honda Y, Honda S. The daf-2 gene network for longevity regulates oxidative stress resistance and Mn-superoxide dismutase gene expression in *Caenorhabditis elegans*. *FASEB J*. 1999;13:1385–1391.
45. Ishii N, Goto S, Hartman P. Protein oxidation during aging of the nematode *Caenorhabditis elegans*. *Free Radic Biol Med*. 2002;33: 1021–1025.
46. Liang H, Masoro EJ, Nelson JF, Strong R, McMahan CA, Richardson A. Genetic mouse models of extended lifespan. *Exp Gerontol*. 2003;38:1353–1364.
47. Murakami S, Salmon A, Miller RA. Multiplex stress resistance in cells from long-lived dwarf mice. *FASEB J*. 2003;17:1565–1566.
48. Andziak B, O'Connor TP, Qi W, et al. High oxidative damage levels in the longest-living rodent, the naked mole-rat. *Aging Cell*. 2006;5:463–471.
49. Schriner SE, Linford NJ, Martin GM, et al. Extension of murine life span by overexpression of catalase targeted to mitochondria. *Science*. 2005;308:1909–1911.
50. Van Remmen H, Ikeno Y, Hamilton M, et al. Lifelong reduction in MnSOD activity results in increased DNA damage and higher incidence of cancer but does not accelerate aging. *Physiol Genomics*. 2003;16:29–37.
51. Elchuri S, Oberley TD, Qi W, et al. Cu/ZnSOD deficiency leads to persistent and widespread oxidative damage and hepatocarcinogenesis later in life. *Oncogene*. 2005;24:367–380.
52. Evans JG, Collins MA, Lake BG, Butler WH. The histology and development of hepatic nodules and carcinoma in C3H/He and C57BL/6 mice following chronic phenobarbitone administration. *Toxicol Pathol*. 1992;40(4):585–594.
53. Pérez V, Bokov A, Van Remmen H, et al. Is the oxidative stress theory of aging dead? *Biochim Biophys Acta*. 2009;1790:1005–1014.
54. Rebrin I, Kamzalov S, Sohal RS. Effects of age and caloric restriction on glutathione redox state in mice. *Free Radic Biol Med*. 2003;35:626–635.
55. Rebrin I, Bayne AC, Mockett RJ, Orr WC, Sohal RS. Free aminothiols, glutathione redox state and protein mixed disulphides in aging Drosophila melanogaster. *Biochem J*. 2004;382:131–136.

56. Rebrin I, Sohal RS. Comparison of thiol redox state of mitochondria and homogenates of various tissues between two strains of mice with different longevities. *Exp Gerontol*. 2004;39:1513–1519.
57. Hansen JM, Go YM, Jones DP. Nuclear and mitochondrial compartmentation of oxidative stress and redox signaling. *Annu Rev Pharmacol Toxicol*. 2006;46:215–234.
58. Hsieh CC, Papaconstantinou J. Thioredoxin-ASK1 complex levels regulate ROS-mediated p38 MAPK pathway activity in livers of aged and long-lived Snell dwarf mice. *FASEB J*. 2006;20:259–268.
59. Surh YJ, Kundu JK, Na HK, Lee JS. Redox-sensitive transcription factors as prime targets for chemoprevention with anti-inflammatory and antioxidative phytochemicals. *J Nutr*. 2005;132:2993S–3001S.
60. Powis G, Mustacich D, Coon A. The role of the redox protein thioredoxin in cell growth and cancer. *Free Rad Biol Med*. 2000;29:312–322.
61. Mahlke MA, Cortez LA, Ortiz MA, et al. The anti-tumor effects of CR are correlated with reduced oxidative stress in ENU-induced gliomas. *Pathobiol Aging Age Relat Dis*. 2011;1:7189. doi:10.3402/pba.v1i0.7189.